AD-A132 276 NULLING WITH LIMITED DEGREES OF FREEDOM(U) ROME AIR DEVELOPMENT CENTER GRIFFISS AFB NY R L HAUPT APR 83 RADC-TR-83-114 1/3

UNCLASSIFIED F/G 20/14 NL

END
DATE FILMED
9 -83
DTIC

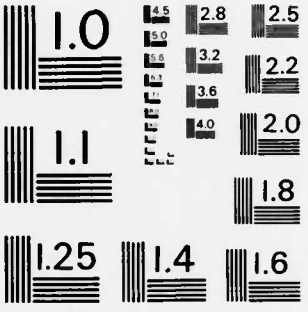

RADC-TR-83-114
In-House Report
April 1983

NULLING WITH LIMITED DEGREES OF FREEDOM

Randy L. Haupt, Captain, USAF

APPROVED FOR PUBLIC RELEASE; DISTRIBUTION UNLIMITED

ROME AIR DEVELOPMENT CENTER
Air Force Systems Command
Griffiss Air Force Base, NY 13441

This report has been reviewed by the RADC Public Affairs Office (PA) and is releasable to the National Technical Information Service (NTIS). At NTIS it will be releasable to the general public, including foreign nations.

RADC-TR-83-114 has been reviewed and is approved for publication.

APPROVED: Philipp Blacksmith

PHILIPP BLACKSMITH
Chief, EM Techniques Branch
Electromagnetic Sciences Division

APPROVED: Allan C. Schell

ALLAN C. SCHELL
Chief, Electromagnetic Sciences Division

FOR THE COMMANDER: John P. Huss

JOHN P. HUSS
Acting Chief, Plans Office

If your address has changed or if you wish to be removed from the RADC mailing list, or if the addressee is no longer employed by your organization, please notify RADC (EECS) Hanscom AFB MA 01731. This will assist us in maintaining a current mailing list.

Do not return copies of this report unless contractual obligations or notices on a specific document requires that it be returned.

Unclassified

SECURITY CLASSIFICATION OF THIS PAGE (When Data Entered)

REPORT DOCUMENTATION PAGE		READ INSTRUCTIONS BEFORE COMPLETING FORM
1. REPORT NUMBER RADC-TR-83-114	2. GOVT ACCESSION NO. A132226	3. RECIPIENT'S CATALOG NUMBER
4. TITLE (and Subtitle) NULLING WITH LIMITED DEGREES OF FREEDOM		5. TYPE OF REPORT & PERIOD COVERED In-House 6. PERFORMING ORG. REPORT NUMBER
7. AUTHOR(s) Randy L. Haupt, Capt., USAF		8. CONTRACT OR GRANT NUMBER(s)
9. PERFORMING ORGANIZATION NAME AND ADDRESS Rome Air Development Center (EEC) Hanscom AFB Massachusetts 01731		10. PROGRAM ELEMENT, PROJECT, TASK AREA & WORK UNIT NUMBERS 62702F 46001507
11. CONTROLLING OFFICE NAME AND ADDRESS Rome Air Development Center (EEC) Hanscom AFB Massachusetts 01731		12. REPORT DATE April 1983 13. NUMBER OF PAGES 46
14. MONITORING AGENCY NAME & ADDRESS(if different from Controlling Office)		15. SECURITY CLASS. (of this report) Unclassified 15a. DECLASSIFICATION/DOWNGRADING SCHEDULE

16. DISTRIBUTION STATEMENT (of this Report)

Approved for public release; distribution unlimited.

17. DISTRIBUTION STATEMENT (of the abstract entered in Block 20, if different from Report)

18. SUPPLEMENTARY NOTES

RADC Project Engineer: Livio Poles, EECS

19. KEY WORDS (Continue on reverse side if necessary and identify by block number)

Adaptive nulling
Partial adaptive nulling
Phased array
Adaptive antenna

20. ABSTRACT (Continue on reverse side if necessary and identify by block number)

A partial adaptive array is a more feasible alternative to the fully adaptive array when the number of array elements becomes very large. Three possible methods of implementing partial adaptive nulling are to place the adaptive controls at (1) selected elements in the aperture, (2) the subarray outputs, or (3) the feed of a space fed array. Of these choices, the first produces much less distortion to the antenna's far field pattern than the other two. This report analyzes the distortions due to nulling with limited degrees of freedom.

DD FORM 1 JAN 73 1473 EDITION OF 1 NOV 65 IS OBSOLETE

Unclassified

SECURITY CLASSIFICATION OF THIS PAGE (When Data Entered)

Preface

I am grateful for the helpful comments and suggestions on subarray nulling provided by Dr. Peter Franchi. I would also like to thank MSgt Dion Shannon for the technical illustrations that appear in this report.

Contents

Illustrations

Illustrations

Tables

Nulling With Limited Degrees of Freedom

I. INTRODUCTION

An adaptive antenna reduces interference to a radar or communication system by placing a null in the far field antenna pattern in the direction of the jamming source. The adaptive antenna must be able to generate M nulls to cancel M jammers in its environment. As long as the number of jammers is less than the number of adaptive elements in a phased array, the necessary nulls can be theoretically generated. A fully adaptive phased array has N elements, with an adaptive control at each element. In this case, the antenna has N-1 degrees of freedom to cancel N-1 jammers.

Adaptive antennas are useful in small communication arrays (4 to 10 elements). The number of adaptive controls for such an array are small. As a result, the added system cost and complexity is reasonable and is often worth the anti-jamming capability.

Unlike communication arrays, radar phased arrays typically have hundreds or thousands of elements. Making such a large phased array fully adaptive has several drawbacks. First, the extra hardware makes the system very complicated. The additional hardware also leads to the problem of increased costs. The expense of developing, operating, and maintaining variable complex weights or receivers at every element becomes exorbitant. A final problem is the adaptation time needed

(Received for publication 2 May 1983)

to cancel the jammers. Radars usually have tight time contraints due to dwell time. Some adaptive algorithms use a random search to find the optimum weight values. The random search algorithms vary the signal at one element at a time to arrive at the optimum antenna pattern. This technique works fine for small arrays, but takes a long time to converge on large arrays. Other algorithms form the signal correlation matrix, then invert the matrix to find the optimum weights. Forming and inverting the correlation matrix of a large array requires nearly perfectly matched receivers at each element. In addition, the matrix is very large and not easily inverted.

Partial adaptive nulling offers solutions to some of the problems associated with large fully adaptive arrays.[1,2] Unlike a fully adaptive array, the partially adaptive array only has T variable controls for nulling, where T < N. Fewer controls means the system is less complex, cheaper, and faster. These advantages are gained through sacrificing "control ability" of the antenna pattern. The fewer adaptive weights in the system, the less the antenna can be controlled. This implies fewer jammers can be canceled, and sidelobe levels are harder to maintain. The tradeoff seems worthwhile, since there are usually many more elements in the array than number of jammers in the environment.

This report looks at null synthesis with limited degrees of freedom. Null synthesis differs from adaptive nulling, because null synthesis is a theoretical, no error, and no feedback process, while adaptive nulling employs feedback to place the nulls in spite of errors. Even though nulls synthesis cannot be practically applied to actual phases arrays, it provides valuable insite into the adaptive process. Also, the null synthesis process described in the following pages can be made adaptive by incorporating a beam orthogonalization procedure and an adaptive algorithm.

Three different types of nulling procedures will be discussed. Each uses a fraction of the total number of elements in the aperture to generate nulls. The type of procedure used depends upon the antenna configuration. The first nulling technique uses only a small portion of the total number of elements. These selected elements have variable complex weights to change the amplitude and phase of the element's signal. A second technique places the variable complex weights at the antenna's subarray level. Thus, there is one complex weight for every subarray. The final nulling process puts the variable complex weights at the feed of a space-fed lens. Each of these null synthesis techniques has fewer degrees of freedom available for nulling, than number of elements in the aperture.

---

1. Chapman, D.J. (1976) Partial adaptivity for the large array. IEEE Trans. on Antennas and Propagation, AP-24(No. 5):685-696.

2. Morgan, D.R. (1978) Partially adaptive array techniques. IEEE Trans. on Antennas and Propagation, AP-26(No. 5):823-833.

2. NULLING WITH SELECTED ELEMENTS

A fully adaptive array has N variable controls for N elements. In most situations, the number of jammers is much less than the number of elements. The logical conclusion to draw is to place only enough variable controls in the array to adequately counter the worst expected jamming scenario. Selecting the proper position and number of elements used in the nulling process determines how well a jammer can be cancelled, while keeping the antenna pattern intact.

The array in Figure 1 serves as the model for analyzing null synthesis with selected elements in the aperture. Each of the array elements has a phase shifter for steering the main beam in the direction of the desired source. Element n has a phase shift of $k d_n u_s$ where

$k = 2\pi/\lambda$,

λ = wavelength,

d_n = distance of element from center of array (in wavelengths),

$u_s = \sin \theta_s$,

θ_s = direction of source from boresite.

Behind each phase shifter is a fixed amplitude weight. These weights have values corresponding to a distribution that generates low sidelobes in the far field antenna pattern. Some typical amplitude distributions are Taylor, Chebychev, and cosine. Elements q1, q2, ... qT have variable complex weights after the fixed amplitude weights. These elements form the nulls in the far field antenna pattern. The variable complex weights have values represented by $1 + \alpha_t + j\beta_t$ for t= q1, q2, ... qT, T < N. Finally, all N signals are added together in the summer to produce a total output signal. When no jammers are in the environment, the total output signal is the sum of the desired signal and internal noise at each element. When interference appears in the environment, the total output signal is the sum of the desired signal, noise, and interference at each element. Changing the amplitude and phase of the variable complex weights affects the total output signal of the array. The weights can be set at certain values so the interference signals cancel, while the desired signal changes very little.[3,4]

---

3. Shore, R.A., and Steyskal, H. (1983) Nulling in Linear Array Patterns With Minimization of Weight Perturbations, RADC-TR-82-32, AD A118695.

4. Haupt, R.L. (1982) Simultaneous Nulling in the Sum and Difference Patterns of a Monopulse Antenna, RADC-TR-82-274.

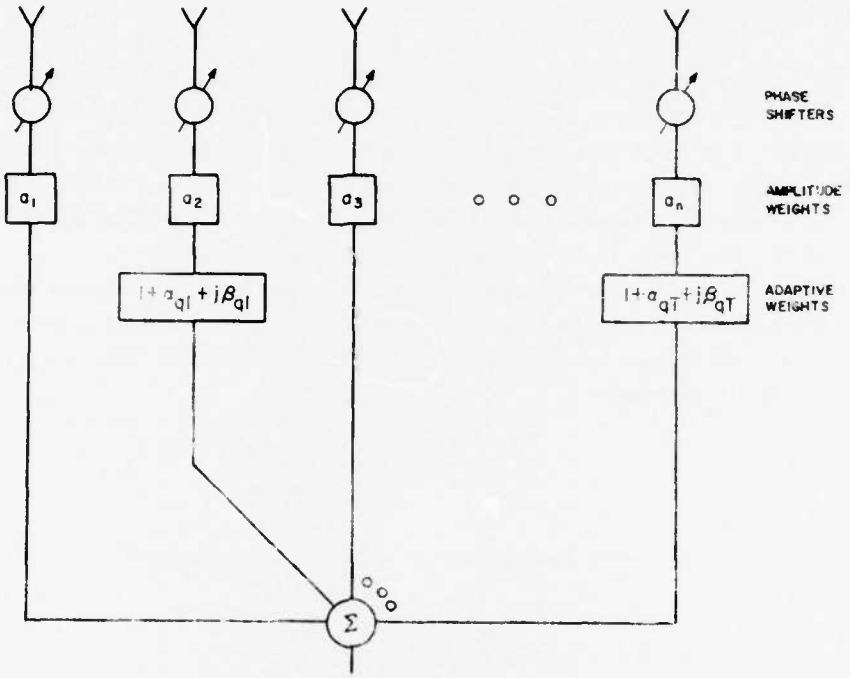

Figure 1. N Element Linear Array With T Adaptive Controls

The quiescent values of the array weights are

$$w_n = a_n \exp[-jk d_n u_s], \quad n = 1, 2, \ldots, N . \tag{1}$$

Here, the variable complex weights, $1 + \alpha_t + \beta_t$ are in their quiescent state $\alpha_t = \beta_t = 0$. Transforming the quiescent weights to the far field results in the far field pattern represented by

$$S(u) = \sum_{n=1}^{N} a_n \exp[jk d_n (u - u_s)]. \tag{2}$$

When jammers appear in the sidelobe regions, the variable complex weights are adjusted to produce a null in the directions of the jammers. Now, the variable complex weights in cascade with the phase shifters and fixed amplitude weights yield

$$w_t = a_t (1 + \alpha_t + j\beta_t) \exp[-jk d_t u_s] \quad t = q1, q2, \ldots, qT . \tag{3}$$

The remaining N-T elements remain unchanged. Transforming the new array weights to the far field produces an antenna pattern represented by

$$S'(u) = \sum_{n=1}^{N} a_n(1 + \alpha_n + j\beta_n) \exp[jk d_n(u - u_s)] \tag{4}$$

and

$$\alpha_n, \beta_n = 0 \text{ when } n \neq qt, \; t = 1, 2, \ldots, T .$$

This pattern has nulls in the direetions of the M jammers (θ_m). In other words, $S(u) = 0$ when $u = u_m$ for $m = 1, 2, \ldots, M$.

$$\sum_{n=1}^{N} a_n \exp[jk d_n(u_m - u_s)] + \sum_{t=q1}^{qT} a_t (\alpha_t + \beta_t) \exp[jk d_t(u_m - u_s)] = 0 \tag{5}$$

$$S(u_m) + \sum_{t=q1}^{qT} a_t (\alpha_t + j\beta_t) \exp[jk d_t(u_m - u_s)] = 0 . \tag{6}$$

Equation (6) is the sum of the quieseent pattern and M eaneellation beams. The sum of the eancellation beams has the same amplitude as the quiescent pattern at the angle θ_m, but is *180° out of phase*.

In order to find the values for α_t and β_t that produee nulls in the direetions of interference, we must solve Eq. (6). This equation is aetually a set of M simultaneous equations with T unknowns. Since there are more unknowns than equations, no unique solution exists for α_t and β_t. Rearranging Eq. (6) into the matrix form $AX = B$ yields

$$\sum_{t=q1}^{qT} a_t(\alpha_t + j\beta_t) \exp[jk d_t(u_m - u_s)] = - \sum_{n=1}^{N} a_n \exp[jk d_n(u_m - u_s)] \tag{7}$$

$$A = \begin{bmatrix} a_{q1} \exp[jk d_{q1}(u_1 - u_s)] & \cdots & a_T \exp[jk d_{qT}(u_1 - u_s)] \\ \vdots & & \vdots \\ a_{q1} \exp[jk d_{q1}(u_m - u_s)] & \cdots & a_T \exp[jk d_{qT}(u_m - u_s)] \end{bmatrix} \tag{8}$$

$$X = \begin{bmatrix} \alpha_{q1} + j\beta_{q1} \\ \vdots \\ \alpha_{qT} + j\beta_{qT} \end{bmatrix} \tag{9}$$

$$B = \begin{bmatrix} -\sum_{n=1}^{N} a_n \exp[jk\, d_n(u_1 - u_S)] \\ \vdots \\ -\sum_{n=1}^{N} a_n \exp[jk\, d_n(u_m - u_S)] \end{bmatrix} . \tag{10}$$

The least mean square solution of $AX = B$ by minimizing $\alpha_n^2 + \beta_n^2$ is

$$X = A^{\dagger} (AA^{\dagger})^{-1} B . \tag{11}$$

$A^{\dagger}$ is the transpose complex conjugate of the matrix A. Solving Eq. (11) for the unknowns α_t and β_t in the matrix X gives

$$\alpha_t = \sum_{m=1}^{M} \left\{ y_m a_t \cos[d_t(u_m - u_s)] + z_m a_t \sin[d_t(u_s - u_m)] \right\} \tag{12}$$

$$\beta_t = \sum_{m=1}^{M} \left\{ -y_m a_t \sin[d_t(u_s - u_m)] + z_m a_t \cos[d_t(u_s - u_m)] \right\} . \tag{13}$$

The variables y_m and z_m are elements in the complex vector Y defined by

$$Y = (AA^{\dagger})^{-1} B . \tag{14}$$

When all the adaptive elements are symmetrically placed about the center of the array, Y is a real matrix.

The array modeled on the computer had 20 elements with a -30 dB, $\bar{n} = 4$ Taylor distribution. Figure 2 shows the array's quiescent far field pattern. Several runs were made using this array model with two and four adaptive elements. The two major questions that need answers are which elements are the best to use and how many elements are needed to adequately perform the nulling.

Figures 3 to 9 show the far field patterns of the model using two adaptive elements and a jammer located at 33°. Along with each nulling pattern is the corresponding cancellation beam superimposed on the quiescent far field pattern. Watching the cancellation beam change as different elements are used for adaptation, gives insite to pattern perturbations due to nulling.

When only two elements in the array are adaptive, they form an interferometer. When the adaptive elements are close together, their resulting cancellation beam is a very broad pattern with only one null. The cancellation beam is the far field pattern of two elements spaced $\lambda/2$ apart. As the adaptive elements are moved apart, the cancellation beam has more peaks and nulls. The number of peaks and

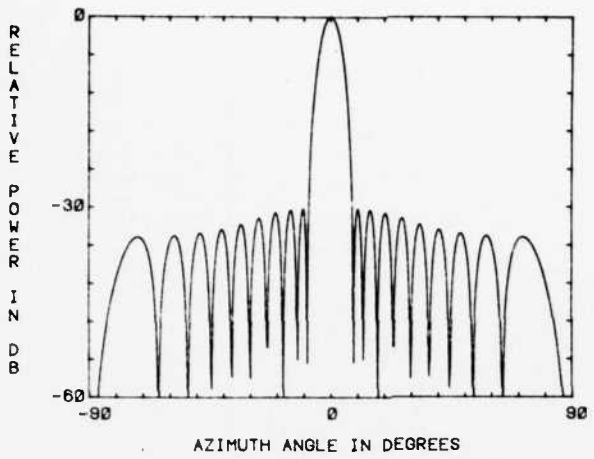

Figure 2. Quiescent Far Field Pattern of a Linear Array With a -30 dB, $\bar{n} = 4$ Taylor Amplitude Distribution

nulls increase until the last element on both ends of the array are used as the adaptive elements. At the extreme ends the cancellation beam has basically the same ripple pattern as the quiescent pattern.

Figures 3a to 4b show some computed results for symmetrically placed adaptive elements in the array. The best results were obtained when the last element on both ends of the array were used for the adaptive elements. In that situation, cancellation was achieved with little perturbation to the rest of the pattern. Symmetrical adaptive elements result in a real Y matrix. The values for the variable complex weights have the same amplitude, but opposite phases. Because of these facts, the far field pattern tends to cancel exactly and add together at different angles. Thus, the new antenna pattern has distinct nulls and the sidelobe structure remains close to the quiescent sidelobe structure.

Unsymmetrical adaptive elements produce a complex Y matrix. The cancellation beam does not have deep nulls and high peaks. Instead, it is a wavy pattern at about the same level as the sidelobes. When the quiescent pattern and cancellation beams are added together, the resultant pattern has "filled in nulls". The pattern is still cancelled at the desired points, but the entire sidelobe structure is distorted. Figures 5a and 5b show examples of an antenna pattern and its associated cancellation beam due to unsymmetrical adaptive elements.

The conclusions drawn in the two adaptive element cases apply to arrays with more adaptive elements. Unsymmetrical adaptive elements have a complex Y matrix and tend to fill in the nulls. Symmetrical adaptive elements keep the sidelobe structure close to the quiescent sidelobe structure. Some of the results obtained with four adaptive elements are shown in Figures 7a to 9b. Symmetrically placing the jammers at both ends of the array give the best results. However, generating up to T-1 adaptive nulls is possible using any combination of T adaptive elements. Table 1 lists the array weights for Figures 2 through 9a.

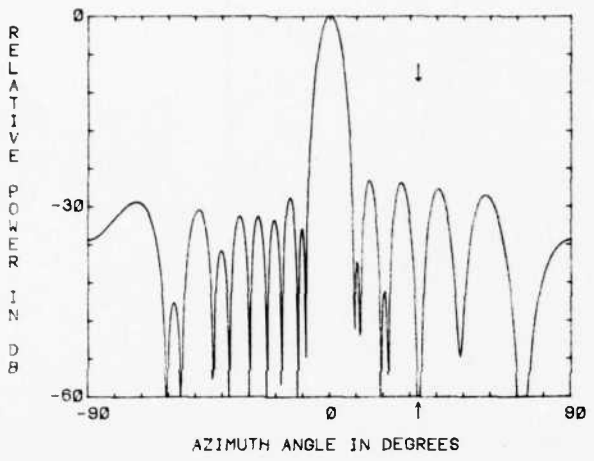

Figure 3a. Far Field Pattern Resulting From Adaptive Controls at Elements 10 and 11 and a Jammer at 33°

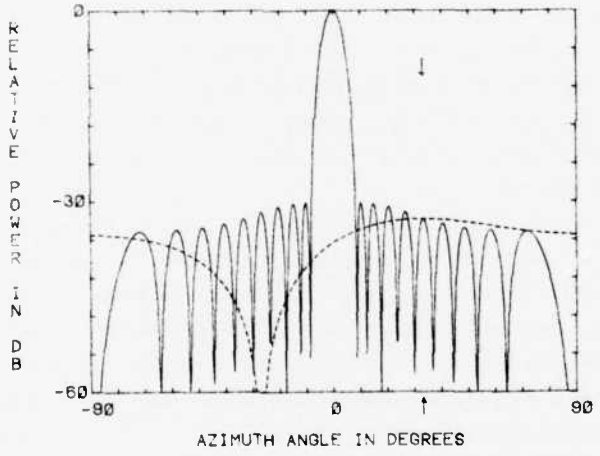

Figure 3b. Cancellation Beam Superimposed on Quiescent Pattern for Adaptive Controls at Elements 10 and 11

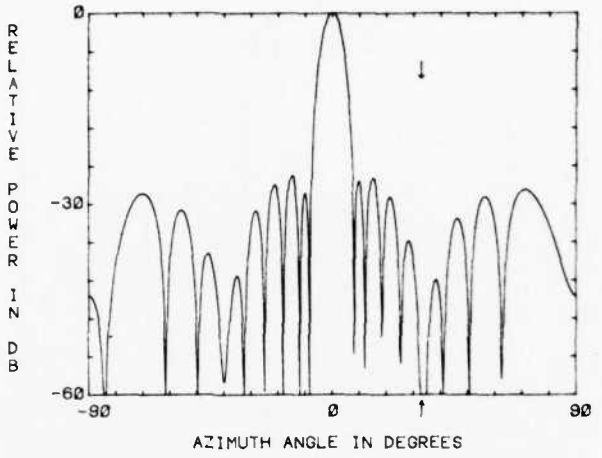

Figure 4a. Far Field Pattern Resulting From Adaptive Controls at Elements 3 and 18 and a Jammer at 33°

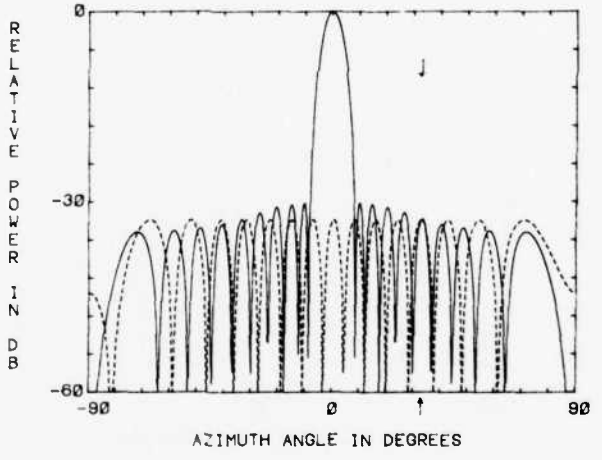

Figure 4b. Cancellation Beam Superimposed on Quiescent Pattern for Adaptive Controls at Elements 1 and 20

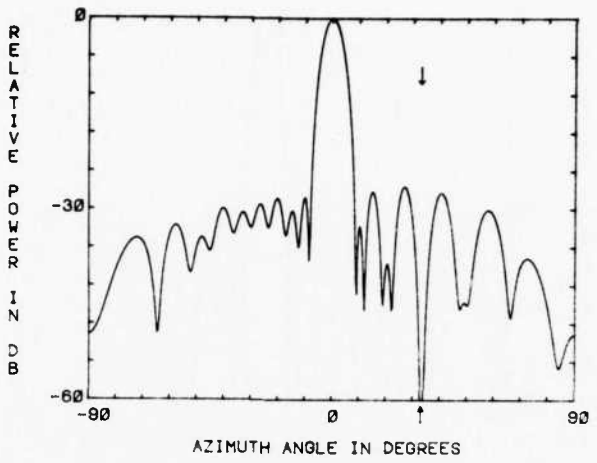

Figure 5a. Far Field Pattern Resulting From Adaptive Controls at Elements 9 and 11 and a Jammer at 33°

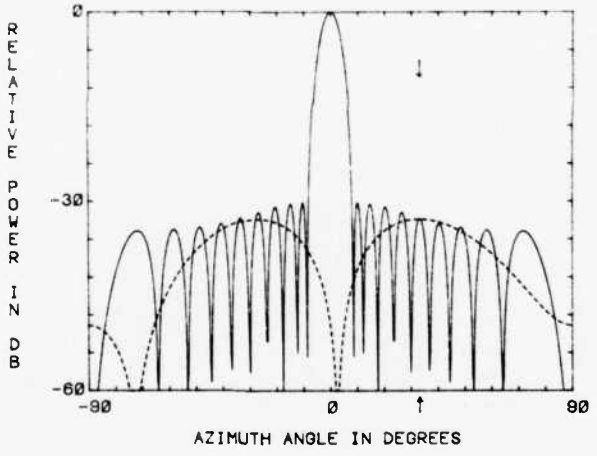

Figure 5b. Cancellation Beam Superimposed on Quiescent Pattern for Adaptive Controls at Elements 9 and 11

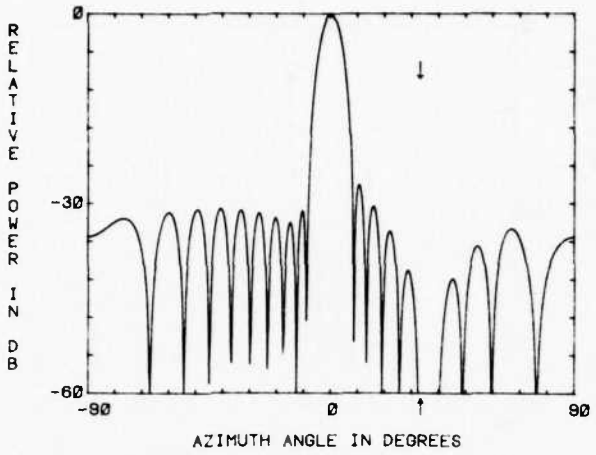

Figure 6a. Far Field Pattern Resulting From Adaptive Controls at Elements 1, 2, 19, 20 and a Jammer at 33°

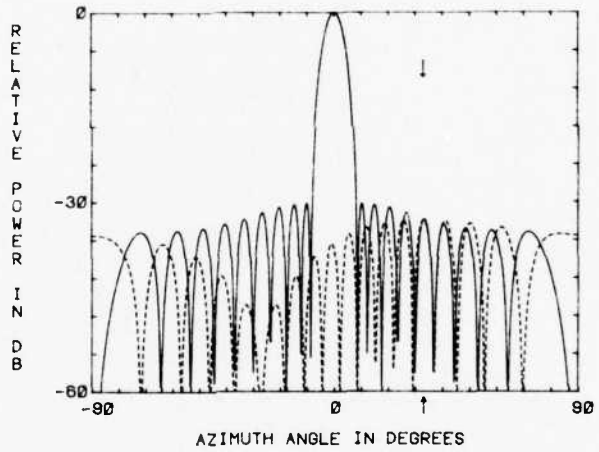

Figure 6b. Cancellation Beam Superimposed on Quiescent Pattern for Adaptive Controls at Elements 1, 2, 19, and 20

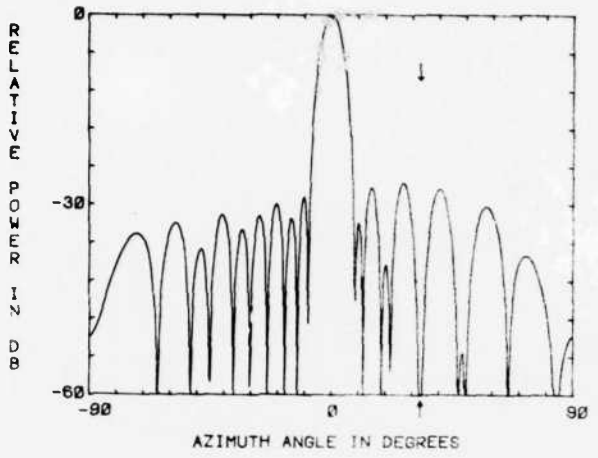

Figure 7a. Far Field Pattern Resulting From Adaptive Controls at Elements 9, 10, 11, 12 and a Jammer at 33°

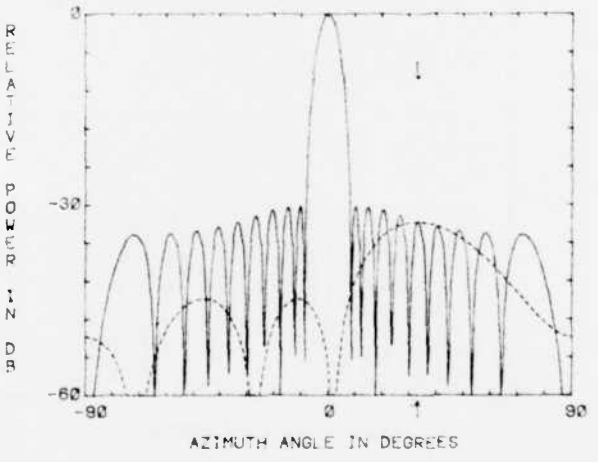

Figure 7b. Cancellation Beam Superimposed on Quiescent Pattern for Adaptive Controls at Elements 9, 10, 11, and 12

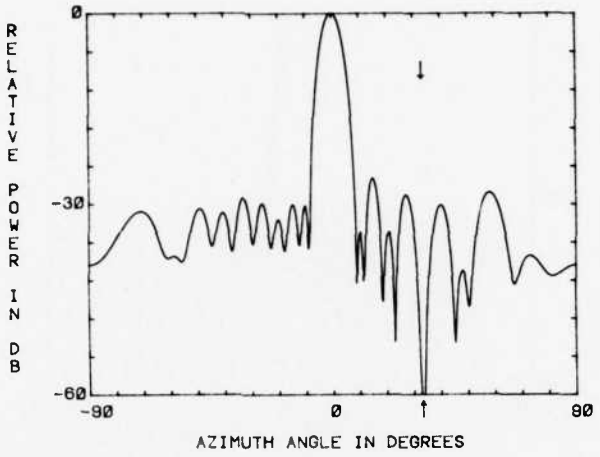

Figure 8a. Far Field Pattern Resulting From Adaptive Controls at Elements 2, 4, 10, 17 and a Jammer at 33°

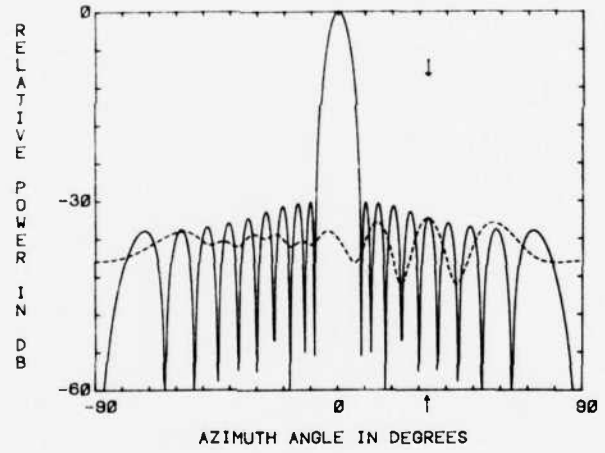

Figure 8b. Cancellation Beam Superimposed on Quiescent Pattern at Elements 2, 4, 10, and 17

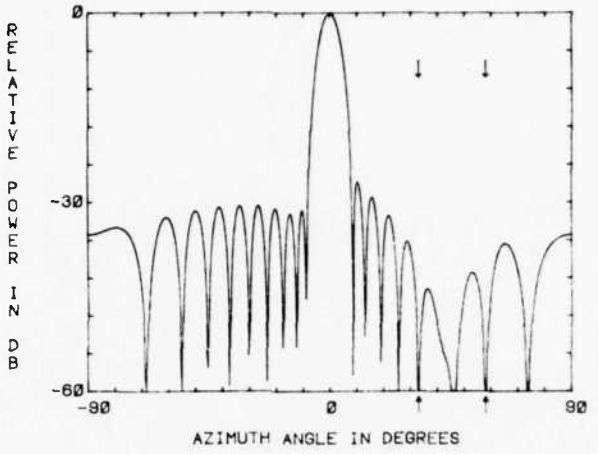

Figure 9a. Far Field Pattern Resulting From Adaptive Controls at Elements 1, 2, 19, 20 and Jammers at 30° and 58°

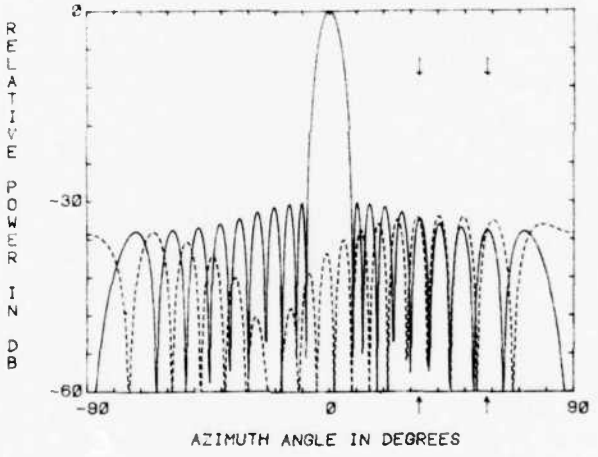

Figure 9b. Cancellation Beam Superimposed on Quiescent Pattern at Elements 1, 2, 19, and 20

Table 1. Product of Taylor Distribution and Variable Complex Weights of Figures 3a to 9a

Element	Quiescent		Figure 3a		Figure 4a		Figure 5a	
	Amp	Ph	Amp	Ph	Amp	Ph	Amp	Ph
1	0.248	0	*		0.144	-0.561		
2	0.294	0						
3	0.378	0						
4	0.487	0						
5	0.605	0						
6	0.721	0						
7	0.824	0						
8	0.909	0						
9	0.969	0						
10	1.000	0	1.102	0.101			0.853	0.091
11	1.000	0	1.102	-0.101				
12	0.969	0					1.106	-0.104
13	0.909	0						
14	0.824	0						
15	0.721	0						
16	0.605	0						
17	0.487	0						
18	0.378	0						
19	0.394	0						
20	0.248	0			0.144	0.561		

When amplitude and phase values are not listed, they are assumed to be the same as the quiescent values. Phases in radians and amplitude values normalized to peak amplitude of quiescent weights.

Table 1. Product of Taylor Distribution and Variable Complex Weights of Figures 3a to 9a (Contd)

Element	Figure 6a		Figure 7a		Figure 8a		Figure 9a	
	Amp	Ph	Amp	Ph	Amp	Ph	Amp	Ph
1	0.198	-0.161					0.184	-0.160
2	0.272	0.295			0.288	0.052	0.306	0.276
3					0.494	-0.090		
4								
5								
6								
7								
8								
9			0.910	0.043				
10			1.051	0.055	1.133	0.126		
11			1.051	-0.055				
12			0.910	-0.043				
13								
14								
15								
16								
17					0.494	0.090		
18							0.306	-0.276
19	0.272	-0.295					0.184	0.160
20	0.198	0.161						

3. NULLING WITH SUBARRAYS

If the antenna has subarrays, then the number of adaptive elements can be reduced by placing a variable complex weight at the output of each subarray. Figure 10 shows a diagram of a linear array with N elements divided into T subarrays. The antenna has N phase shifters and fixed amplitude weights, and T time delays and variable complex weights. The subarrays may or may not contain an equal number of elements. Both cases will be considered.

The quiescent array weights are given by

$$w_n = a_n \exp[-jk d_n u_s] . \tag{15}$$

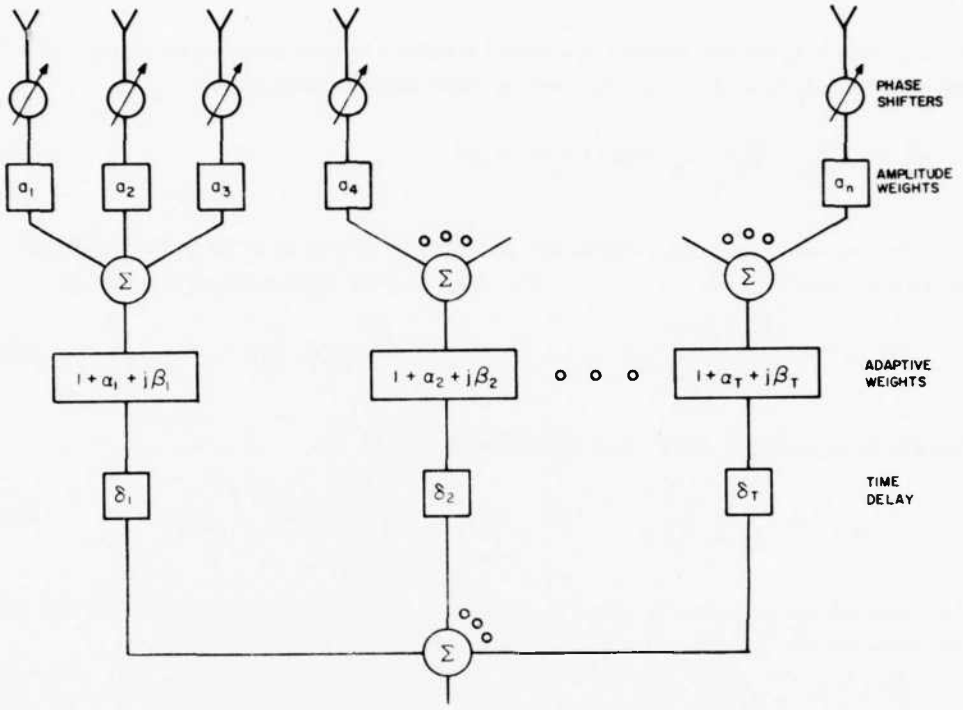

Figure 10. N Element Linear Array With T Subarrays and an Adaptive Weight at Each Subarray

A uniform plane wave incident on the aperture induces a signal level at each element represented by

$$s_n = a_n \exp[jk d_n(u - u_s)] \qquad n = 1, 2, \ldots, N . \tag{16}$$

These weights are added together at the subarray level to give T different outputs.

$$S_t = \sum_{q = Q_t} a_q \exp[jk d_q(u - u_s)] \tag{17}$$

Q_t = set of indices of the element in subarray t

$t = 1, 2, \ldots, T .$

In turn, the T subarray outputs are added together to give one output signal. Under quieseent conditions ($\alpha_t = \beta_t = 0$), the far field antenna pattern is

$$S(u) = \sum_{t=1}^{T} \sum_{q=Q_t} a_q \exp[j(k d_q (u - u_s))] . \tag{18}$$

The variable complex weights are adjusted to ereate M nulls in the far field pattern at angles θ_m (m = 1, 2, ..., M). The new far field pattern is given by

$$S'(u) = 0 = \sum_{t=1}^{T} \sum_{q=Q_t} (1 + \alpha_t + j\beta_t) a_q \exp[j(k d_q (u - u_s)] . \tag{19}$$

The far field pattern, S'(u), has M nulls at $\theta = \theta_m$.

$$S'(u_m) = 0 = \sum_{t=1}^{T} \sum_{q=Q_t} (1 + \alpha_t + j\beta_t) a_q \exp[j(k d_q (u_m - u_s))] . \tag{20}$$

Rearranging this equat.on to put it in the form of M simultaneous equations with T unknowns on the left side and M known quantities on the right yields

$$\sum_{t=1}^{T} \sum_{q=Q_t} a_q (\alpha_t + j\beta_t) \exp[j(k d_q (u_m - u_s))] \tag{21}$$

$$= - \sum_{t=1}^{T} \sum_{q=Q_t} a_q \exp[j(k d_q (u_m - u_s))] . \tag{22}$$

As in the previous section, these equations may be put into the matrix form AX = B and solved using a least mean square fit.

$$A = \begin{bmatrix} \sum_{q=Q_1} a_q \exp\left\{ j[k d_q (u_1 - u_s)] \right\} & \cdots & \sum_{q=Q_T} a_q \exp\left\{ j[k d_q (u_1 - u_s)] \right\} \\ \vdots & & \\ \sum_{q=Q_1} a_q \exp\left\{ j[k d_q (u_m - u_s)] \right\} & \cdots & \sum_{q=Q_T} a_q \exp\left\{ j[k d_q (u_m - u_s)] \right\} \end{bmatrix} \tag{23}$$

$$X = \begin{bmatrix} \alpha_1 + j\beta_1 \\ \vdots \\ \alpha_T + j\beta_T \end{bmatrix} \tag{24}$$

$$B = \begin{bmatrix} -\sum_{t=1}^{T} \sum_{q=Q_t} a_q \exp\left\{ j[k d_q (u_1 - u_2)] \right\} \\ \vdots \\ -\sum_{t=1}^{T} \sum_{q=Q_t} a_q \exp\left\{ j[k d_q (u_m - u_s)] \right\} \end{bmatrix} . \quad (25)$$

The X matrix is given by Eq. (11) and the Y matrix by Eq. (13). Solving for X leads to the following values for α_t and β_t:

$$\alpha_t = \sum_{m=1}^{M} \sum_{q=Q_t} \left\{ y_m a_q \cos[d_q (u_s - u_m)] + z_m a_q \sin[d_q (u_s - u_m)] \right\} \quad (26)$$

$$\beta_t = \sum_{m=1}^{M} \sum_{q=Q_t} \left\{ y_m a_q \sin[d_q (u_s - u_m)] + z_m a_q \cos[d_q (u_s - u_m)] \right\} . \quad (27)$$

These values of the complex variable weights produce nulls in the subarray antenna's far field pattern.

The computer model was an array with 20 elements and a -30 dB, $\bar{n} = 4$ Taylor distribution. Several different subarraying configurations were tried. The first run had only two subarrays (Figure 11a). In every case nulling in the desired direction was adequately achieved. Figures 11a to 19b show the results of nulling with subarrays. The cancellation beam tended to significantly enhance some sidelobes, while significantly reducing others. Symmetry created a real Y matrix, hence the antenna's pattern's nulls were not filled in.

Splitting up the subarrays so that one contained more elements than the other, degraded the far field pattern. The Y matrix is no longer real and the cancellation beam and quiescent pattern add to zero at only a few points. Figure 13a shows the results of nulling with two subarrays, one with 8 elements and the other with 12 elements. Pattern distortion gets progressively worse as the subarray imbalance gets worse.

Varying the number of subarrays and number of elements in a subarray produced considerably different results. In all cases the more subarrays, the better the results. This conclusion makes sense, because the number of controls increases with the number of subarrays. A second way to improve nulling results is to have an equal number of elements in every subarray. Finally, having symmetrical subarrays with equal number of elements produce better results than unsymmetric subarrays. Figures 14a to 16b demonstrate the above observations. Table 2 lists the subarray weights for Figures 11a to 16a.

The null's angular location determines the distortion of the quiescent far field pattern. For instance, a null placed at the peak of a quiescent pattern sidelobe produces more distortion than a null placed near a null in the quiescent pattern. This type of distortion makes sense because more power is needed to cancel a high sidelobe value than a low sidelobe value. The cancellation beam must be raised to the level of the quiescent pattern in the direction of the desired null to produce cancellation. The higher the level of the quiescent pattern, the higher the cancellation beam is raised. Raising the cancellation beam at one point raises it at all points. Thus, the cancellation beam has more impact on the quiescent pattern at all angles. This type of distortion occurs in fully adaptive arrays as well as partially adaptive arrays.

Figures 17a to 17b demonstrate pattern distortion that is dependent upon the sidelobe level of the quiescent pattern. A twenty element uniformly weighted aperture with four equal subarrays was used in these examples. At 10° the quiescent pattern is -18 dB below the peak of its main beam. In order to produce a null at 10°, the cancellation beam is raised to match the quiescent pattern at that angle. The level of the entire cancellation beam goes up. As a result, the sidelobes and mainbeam of the quiescent pattern are distorted. The reduction in the main beam gain is due to 14.4 percent reduction in the amplitude of subarrays 1 and 4 as well as the phase changes of each subarray (see Table 2).

Figure 19a shows the results when the null is placed at 11° instead of 10°. The quiescent pattern at 11° is -27 dB below the peak of the main beam. Nulling at 11° has no noticeable effect on the gain of the main beam. The reason (Figure 19b) is the cancellation beam is only raised to the level of the quiescent pattern at 11°. Since this level is considerably lower than the pattern level at 10°, the resulting pattern distortion is less.

Subarray nulling produces an additional distortion not found in nulling with selected elements. The distortion occurs because the cancellation beam has a limited scan. Consequently, the cancellation is usually done with the sidelobes of the cancellation beam. Raising the sidelobes of the cancellation beam to the level of the quiescent pattern also raises the peak of the cancellation beam. Since the peak is somewhere in the vicinity of the main beam, main beam distortion results.

Nulling with selected elements uses the peak of the cancellation to match the quiescent pattern in the direction of the desired null. As a result, the cancellation beam's sidelobes produce little changes to the quiescent pattern. This fact is evident in the results shown in the previous section.

Table 2 shows the amplitude and phase settings for the subarray variable complex weights in Figures 17a-19a. Notice the large amplitude and phase deviations required to place the null at 60°. The quiescent pattern is -27 dB below the main beam at both 11° and 60°. Since the null at 11° is produced by a peak in the cancellation beam, less distortion results. On the other hand, the null at 60° is generated by a sidelobe of the cancellation beam and significant distortion results.

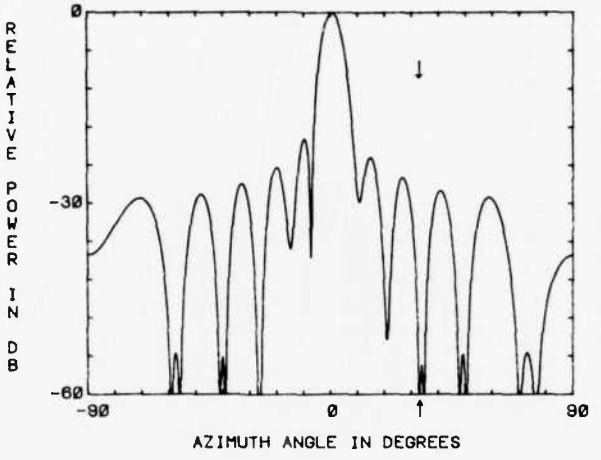

Figure 11a. Far Field Pattern Resulting From Adaptive Controls at 2 Subarrays (10, 10 elements) and a Jammer at 33°

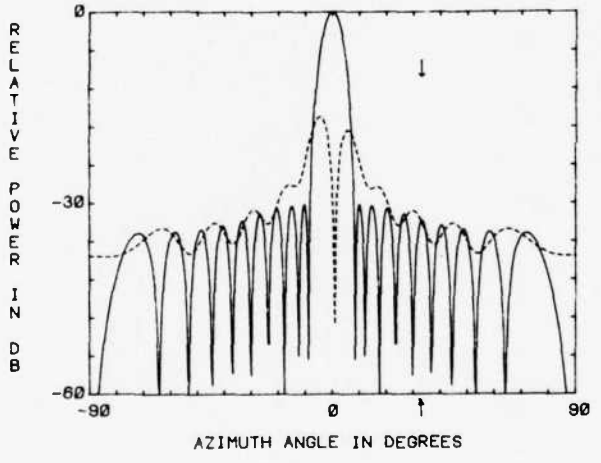

Figure 11b. Cancellation Beam Superimposed on Quiescent Pattern for Adaptive Controls at 2 Subarrays (10, 10 elements)

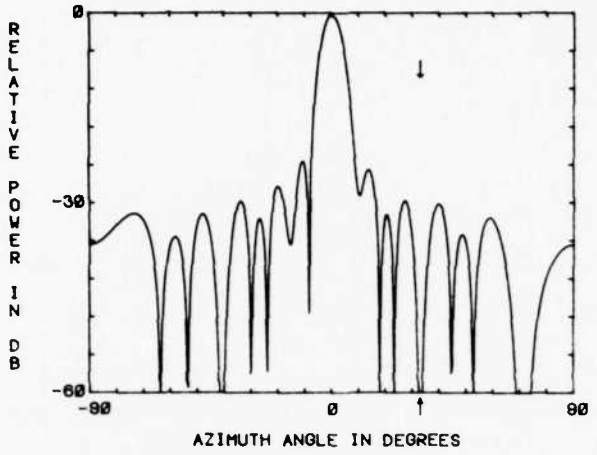

Figure 12a. Far Field Pattern Resulting From Adaptive Controls at 4 Subarrays (5, 5, 5, 5 elements) and a Jammer at 33°

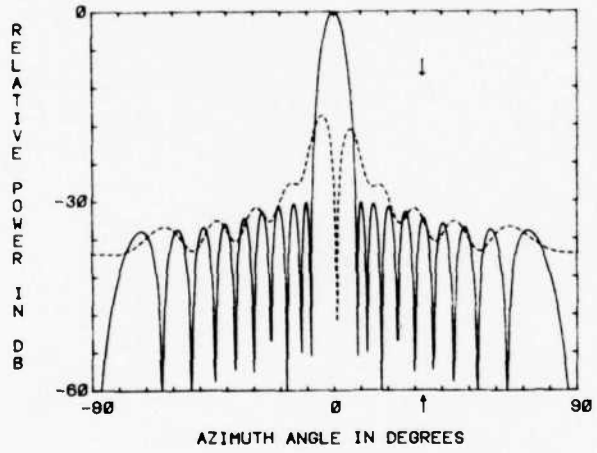

Figure 12b. Cancellation Beam Superimposed on Quiescent Pattern for Adaptive Controls at 4 Subarrays (5, 5, 5, 5 elements)

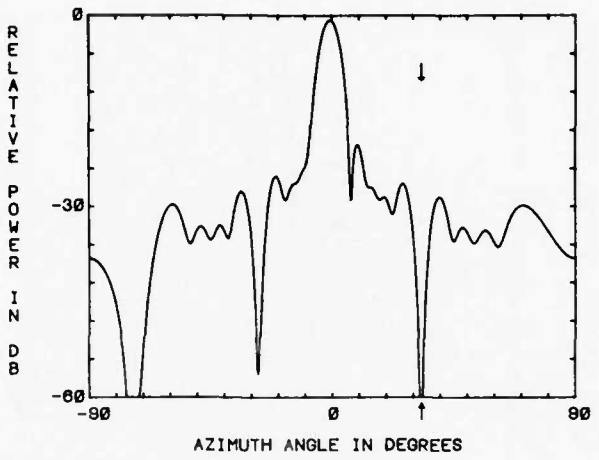

Figure 13a. Far Field Pattern Resulting From Adaptive Controls at 2 Subarrays (8, 12 elements) and a Jammer at 33°

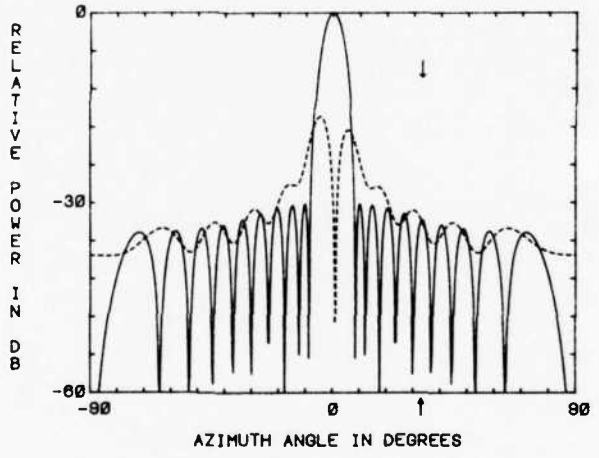

Figure 13b. Cancellation Beam Superimposed on Quiescent Pattern for Adaptive Controls at 2 Subarrays (8, 12 elements)

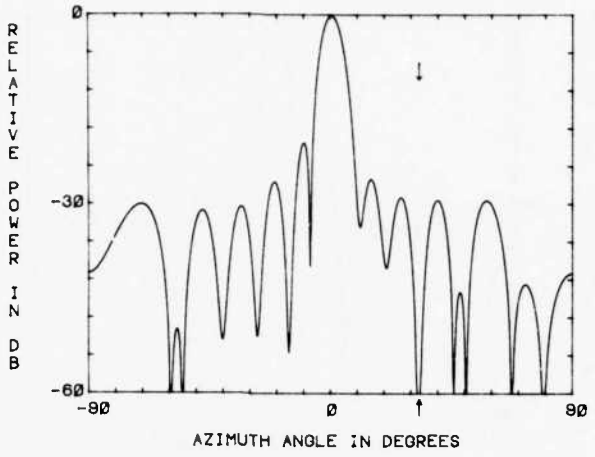

Figure 14a. Far Field Pattern Resulting From Adaptive Controls at 4 Subarrays (2, 8, 8, 2 elements) and a Jammer at 33°

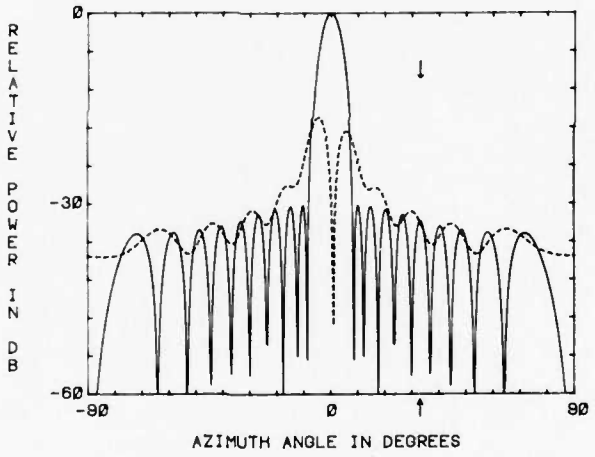

Figure 14b. Cancellation Beam Superimposed on Quiescent Pattern for Adaptive Controls at 4 Subarray (2, 8, 8, 2 elements)

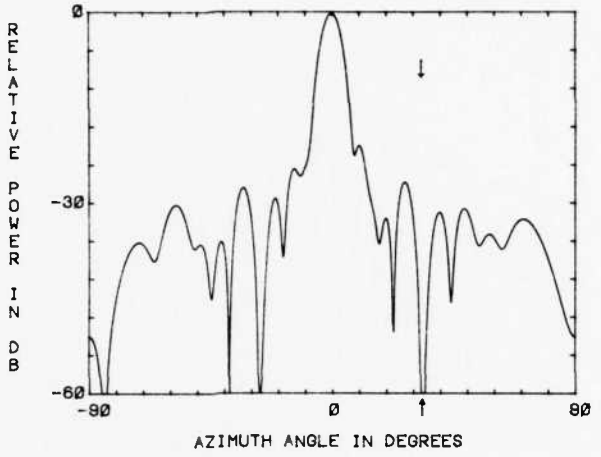

Figure 15a. Far Field Pattern Resulting From Adaptive Controls at 4 Subarrays (2, 4, 6, 8 elements) and a Jammer at 33°

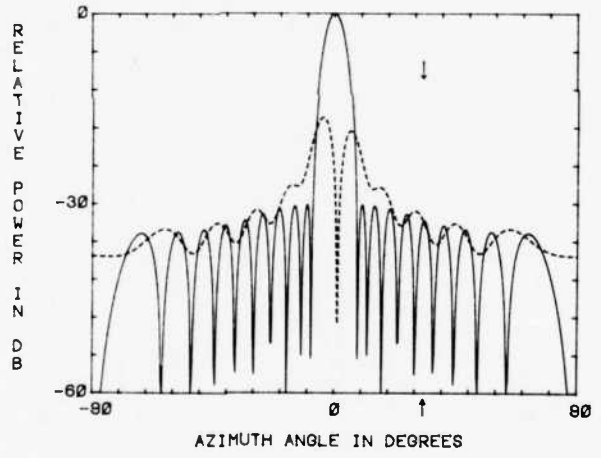

Figure 15b. Cancellation Beam Superimposed on Quiescent Pattern for Adaptive Controls at (2, 4, 6, 8 elements)

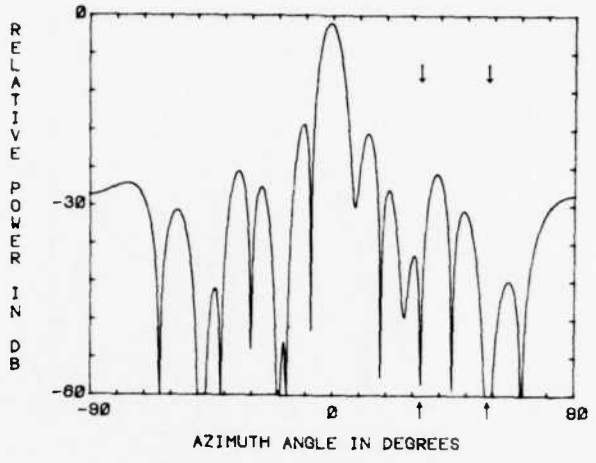

Figure 16a. Far Field Pattern Resulting From Adaptive Controls at 4 Subarrays (5, 5, 5, 5 elements) and Jammers at 33° and 58°

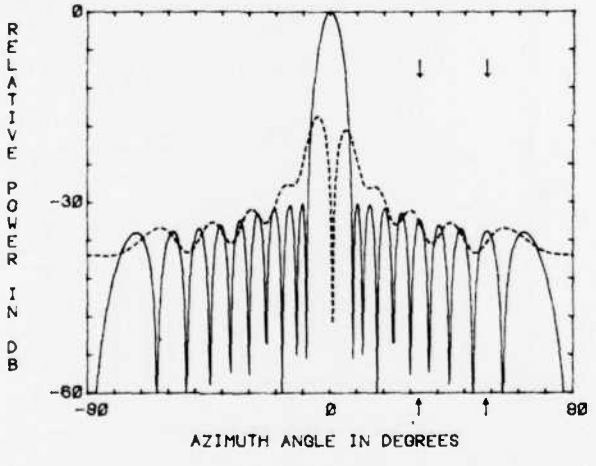

Figure 16b. Cancellation Beam Superimposed on Quiescent Pattern for Adaptive Controls at 4 Subarrays (5, 5, 5, 5 elements) and 2 Jammers

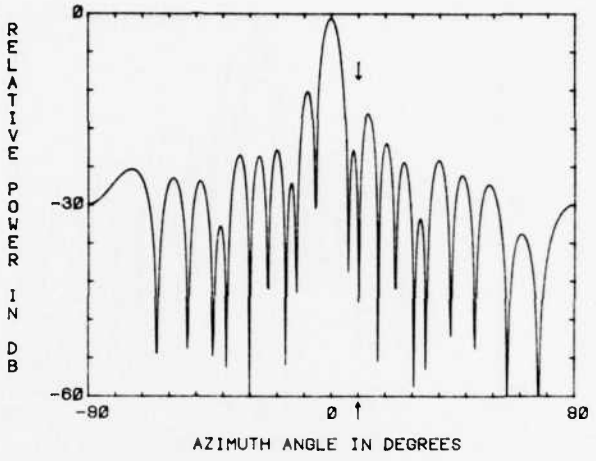

Figure 17a. Uniform Far Field Pattern Resulting From Adaptive Controls at 4 Subarrays (5, 5, 5, 5 elements) and a Jammer at 10°

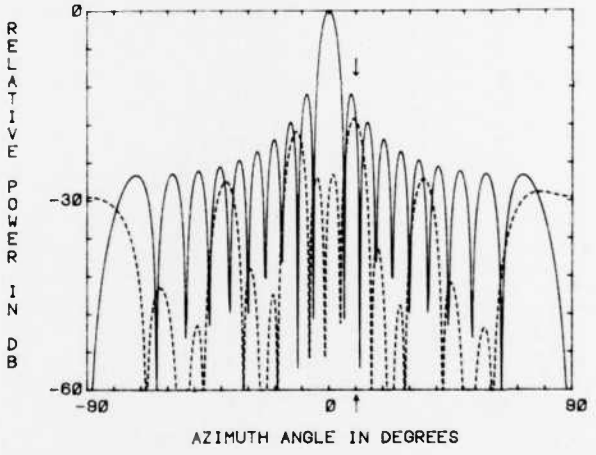

Figure 17b. Cancellation Beam Superimposed on Quiescent Pattern for Adaptive Controls at 4 Subarrays (5, 5, 5, 5 elements)

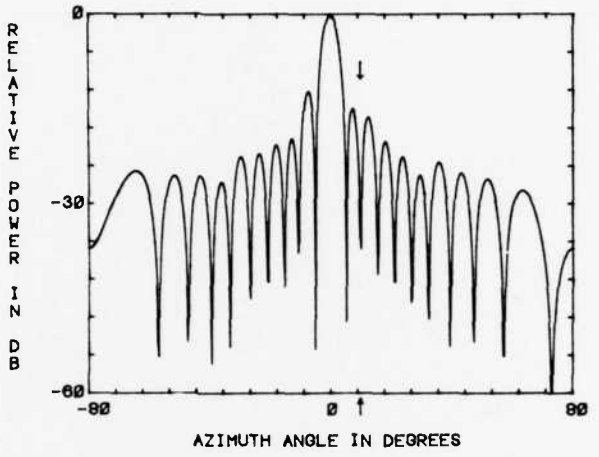

Figure 18a. Uniform Far Field Pattern Resulting From Adaptive Controls at 4 Subarrays (5, 5, 5, 5 elements) and a Jammer at 11°

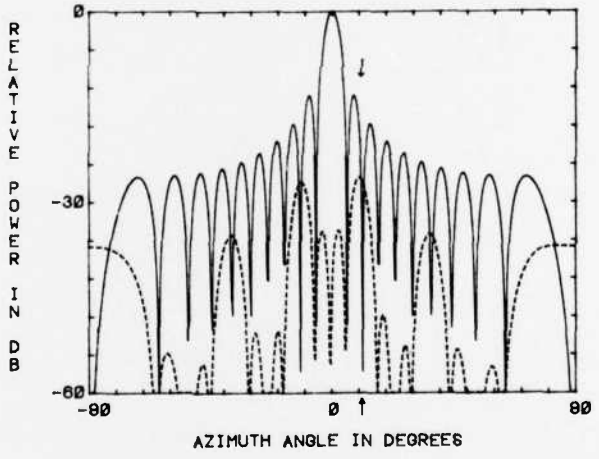

Figure 18b. Cancellation Beam Superimposed on Quiescent Pattern for Adaptive Controls at 4 Subarrays (5, 5, 5, 5 elements)

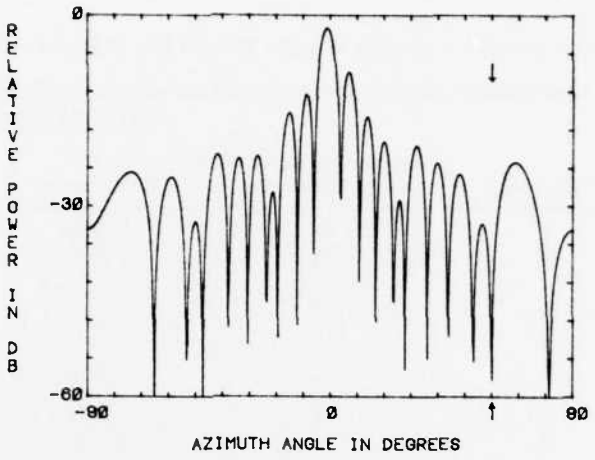

Figure 19a. Uniform Far Field Pattern Resulting From Adaptive Controls at 4 Subarrays (5, 5, 5, 5 elements) and a Jammer at 60°

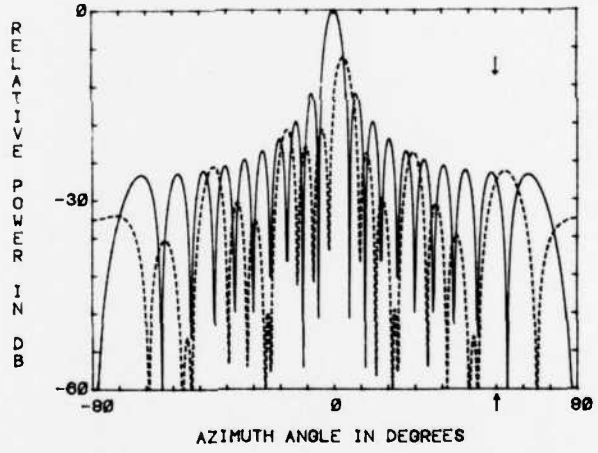

Figure 19b. Cancellation Beam Superimposed on Quiescent Pattern for Adaptive Controls at 4 Subarrays (5, 5, 5, 5 elements)

Table 2. Variable Complex Weight Values for Figures 11a to 19a

Figure	Subarray	Number of Elements in a Subarray	Variable Complex Weights	
			Amplitude	Phase
11a	1	10	1.000	0.208
	2	10	1.000	-0.208
12a	1	5	0.902	-0.208
	2	5	1.000	0.100
	3	5	1.000	-0.100
	4	5	0.902	0.028
13a	1	8	1.028	-0.217
	2	12	0.912	0.246
14a	1	2	0.838	0.049
	2	8	1.000	0.164
	3	8	1.000	-0.164
	4	2	0.838	-0.049
15a	1	2	0.915	0.025
	2	4	0.960	0.058
	3	6	1.000	-0.177
	4	8	0.976	0.099
16a	1	5	1.000	-0.454
	2	5	0.832	0.071
	3	5	0.832	-0.071
	4	5	1.000	0.454
17a	1	5	0.857	-0.170
	2	5	1.000	0.175
	3	5	1.000	-0.175
	4	5	0.857	0.170
18a	1	5	0.980	-0.071
	2	5	1.000	0.071
	3	5	0.980	-0.071
	4	5	1.000	0.071
19a	1	5	1.000	-0.418
	2	5	0.602	-0.341
	3	5	0.602	0.341
	4	5	1.000	0.418

Phase in radians

4. NULLING AT THE FEED OF A SPACE FED LENS

Nulling at the feed of a space fed lens is similar to nulling at the subarrays of an antenna. The space fed lens antenna is a form of subarraying. Each element in the feed contributes power to each element in the lens. This arrangement means the entire lens is a subarray for every feed element. In other words, the number of elements in the lens equals the number of elements in a subarray. The term "totally overlapped subarrays" describes this configuration.

Figure 20 shows a diagram of a space fed lens. Both the feed and the lens are linear arrays of isotropic elements. The lens has N elements and the feed T elements. Every lens element has a variable phase shifter for steering the main beam. In addition, there are N fixed phase shifters to correct for the spherical wave front of the feed. No fixed or variable amplitude weights exist at the lens. Amplitude weighting for low sidelobes is done at the feed.

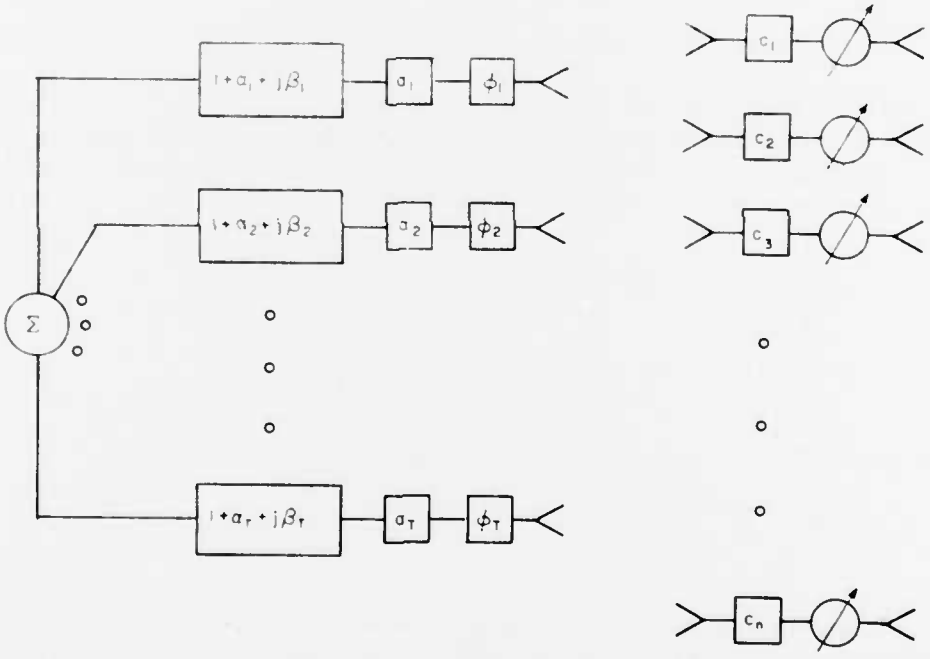

Figure 20. Space Fed Lens With an N Element Lens and T Element Feed

The feed has two sets of complex weights. The first set has fixed values for producing a low sidelobe distribution for the lens. The second set is variable for nulling. These weights are adjusted to produce a null in the far field pattern of the antenna in some desired direction.

The expression for the far field pattern of a space fed lens is slightly more complicated than the other antenna configurations discussed so far. Since the antenna is reciprocal we can pretend it is transmitting or receiving to derive its quiescent far field pattern. In this case we will say the antenna is transmitting. The field distribution on the back of the lens at lens element number n is given by

$$S_n = \sum_{t=1}^{T} \frac{a_t}{R_{nt}} \exp[-j\phi_t] \exp[jkR_{nt}] \tag{28}$$

R_{nt} - distance between feed element t and lens element n (in λ),

a_t - fixed amplitude weight at feed element t,

d_t - fixed phase weight at feed element t.

The signal S_n passes through the fixed phase shifters C_n in the lens that correct for the spherical phase front. In addition, the variable phase shifters impose a linear phase shift $kd\,u_s$ across the array to steer the main beam. When the signal reaches the front side of the array, it has a value of

$$S_n' = \sum_{t=1}^{T} \frac{a_t}{R_{nt}} \exp[j(kR_{nt} - \phi_t)] \exp[-j(C_n + kd_n u_s)] \tag{29}$$

$$= \sum_{t=1}^{T} \frac{a_t}{R_{nt}} \exp[j(kR_{nt} - \phi_t - C_n - kd_n u_s)] . \tag{30}$$

Taking these weights and transforming to the far field leads to Eq. (31),

$$S(u) = \sum_{n=1}^{N} \sum_{t=1}^{T} \frac{a_t}{R_{nt}} \exp[j(kR_{nt} + kd_n u - \phi_t - C_n - kd_n u_s)] . \tag{31}$$

This equation changes in the presence of jammers. Now, the complex variable weights are adjusted to put nulls in the directions of the jammers. The new antenna pattern is zero at the angles θ_m.

$$S'(u_m) = \sum_{n=1}^{N} \sum_{t=1}^{T} \frac{a_t}{R_{nt}} (1 + \alpha_t + j\beta_t) \exp[j(k R_{nt} + k d_n u_m - \phi_t - C_n - k d_n u_s)] = 0 \tag{32}$$

$$\sum_{n=1}^{N} \sum_{t=1}^{T} \frac{a_t}{R_{nt}} (\alpha_t + j\beta_t) \exp[j(R_{nt} + k d_n u_m - \phi_t - C_n - k d_n u_s)]$$

$$= - \sum_{n=1}^{N} \sum_{t=1}^{T} \frac{a_t}{R_{nt}} \exp[j(k R_{nt} + k d_n u_m - \phi_t - C_n - k d_n u_s)] . \tag{33}$$

Equation (23) can be put in the matrix form AX = B where

$$A = \begin{bmatrix} \sum_{n=1}^{N} \delta_{n1} \exp[j\epsilon_{n11}] & \cdots & \sum_{n=1}^{N} \delta_{nT} \exp[j\epsilon_{nT1}] \\ \vdots & & \vdots \\ \sum_{n=1}^{N} \delta_{n1} \exp[j\epsilon_{n1M}] & \cdots & \sum_{n=1}^{N} \delta_{nT} \exp[j\epsilon_{nTM}] \end{bmatrix} \tag{34}$$

$$X = \begin{bmatrix} \alpha_1 + j\beta_1 \\ \vdots \\ \alpha_T + j\beta_T \end{bmatrix} \tag{35}$$

$$B = \begin{bmatrix} \sum_{n=1}^{N} \sum_{t=1}^{T} \delta_{nt} \exp(j\epsilon_{nt1}) \\ \vdots \\ \sum_{n=1}^{N} \sum_{t=1}^{T} \delta_{nt} \exp(j\epsilon_{ntM}) \end{bmatrix} \tag{36}$$

$$\delta_{nt} = \frac{a_t}{R_{nt}} \tag{37}$$

$$\epsilon_{ntm} = k R_{nt} + k d_n u_m - \phi_t - C_n - k d_n u_s . \tag{38}$$

These equations are solved using a least mean square solution.

$$Y = (AA^{\dagger})^{-1} B \tag{39}$$

$$X = A^{\dagger} Y . \tag{40}$$

Y is a complex vector with elements $y_m + j z_m$. The unknown values for α_t and β_t are given by

$$\alpha_t = \sum_{m=1}^{M} \sum_{n=1}^{N} \delta_{n1} \left[y_m \cos(\epsilon_{n1m}) + z_m \sin(\epsilon_{n1m}) \right] \tag{41}$$

$$\beta_t = \sum_{m=1}^{M} \sum_{n=1}^{N} \delta_{n1} \left[-y_m \sin(\epsilon_{n1m}) + z_m \cos(\epsilon_{n1m}) \right] . \tag{42}$$

The space fed lens simulation had a 20-element lens and an f/d of one. Figure 21a shows the results of nulling with a two-element feed. Pattern distortion decreases as the number of feed elements increases. Note that the cancellation beam has a peak in the main beam of the quiescent pattern. The subarray distortion discussed in the last section applies here too. This causes problems when the number of jammers is almost the same as the number of feed elements. The cancellation beam takes away substantial gain from the quiescent pattern's main beam. The results from nulling at the feed of a space fed lens are shown in Figures 21a-23b and Table 3.

Partial adaptive nulling is a feasible approach to nulling in very large arrays. The number of adaptive controls depends upon the interference. The more jammers and wider the system and jammer instantaneous bandwidths, the more adaptive controls that are needed to provide adequate cancellation. In most cases, a fully adaptive array is an overkill and a partially adaptive array provides the necessary nulling with a small amount of pattern distortion.

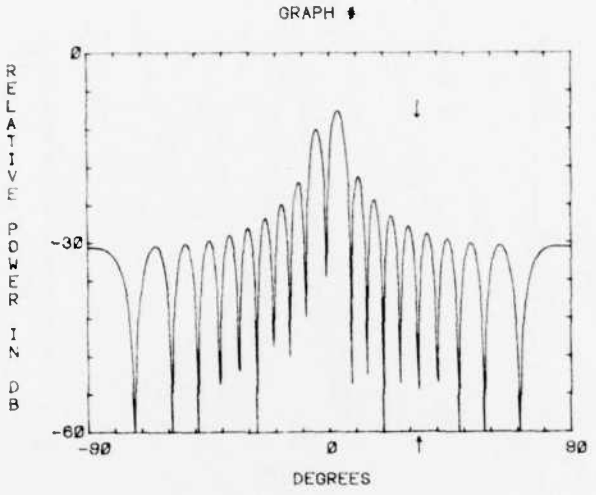

Figure 21a. Far Field Pattern of a Space-Fed Lens With 2 Adaptive Elements in the Feed and 1 Jammer at 33°

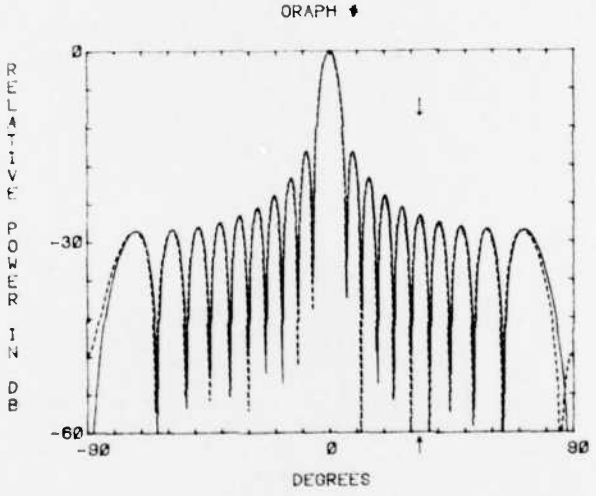

Figure 21b. Cancellation Beam Superimposed on Quiescent Pattern for Adaptive Controls at 2 Feed Elements

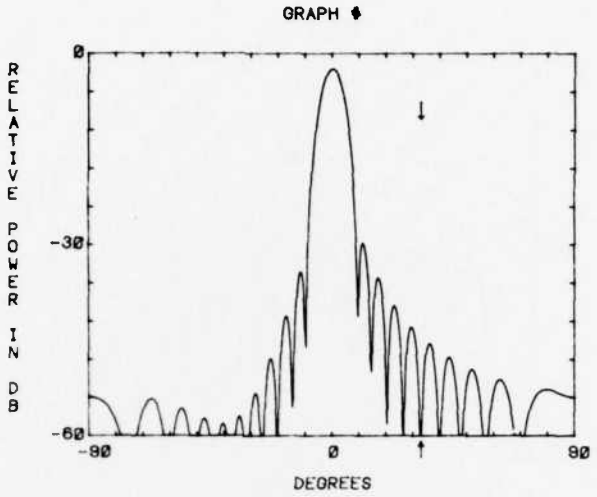

Figure 22a. Far Field Pattern of a Space-Fed Lens With 4 Adaptive Feed Elements and 1 Jammer at 33°

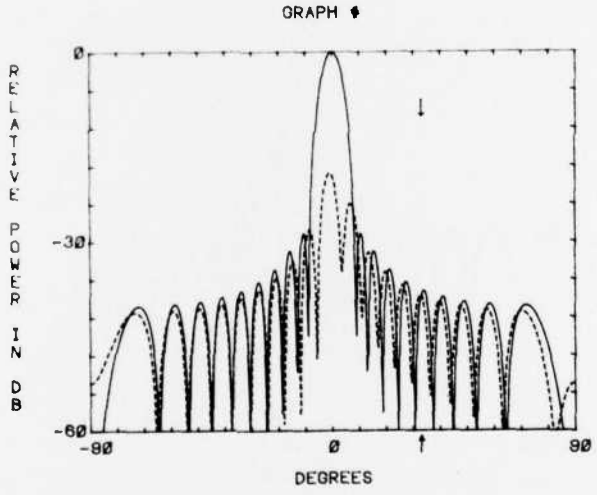

Figure 22b. Cancellation Beam Superimposed on Quiescent Pattern for Adaptive Controls at 4 Feed Elements

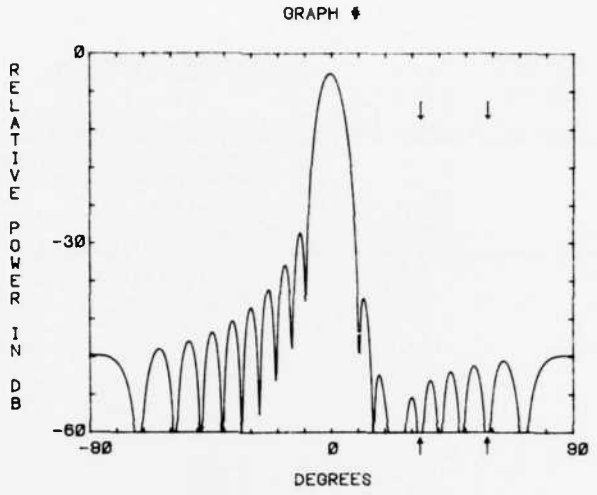

Figure 23a. Far Field Pattern of a Space-Fed Lens With 4 Adaptive Feed Elements and Jammers at 33° and 58°

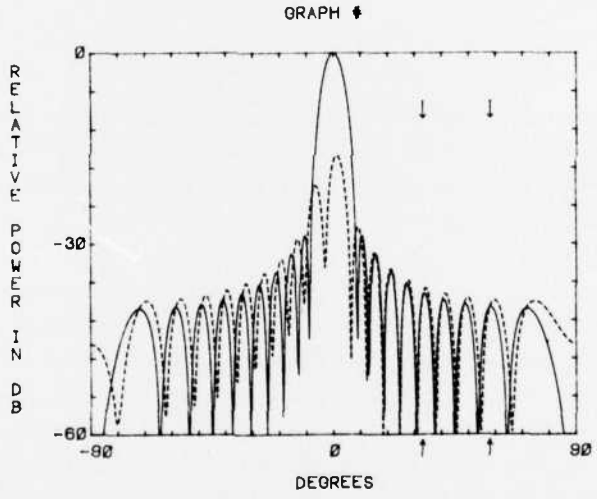

Figure 23b. Cancellation Beam Superimposed on Quiescent Pattern for Adaptive Controls at 4 Feed Elements and 2 Jammers

Table 3. Variable Complex Weight Values for Figures 21a to 23a

Figure	Feed Element	Variable Complex Weights	
		Amplitude	Phase
21a	1	0.773	3.121
	2	1.000	-0.016
22a	1	1.000	-0.085
	2	0.693	0.033
	3	0.603	0.125
	4	0.906	-0.015
23a	1	0.883	-0.107
	2	1.000	-0.002
	3	0.907	0.095
	4	0.807	0.013

Phase in radians

5. CONCLUSIONS

This report analyzed three different methods of nulling with limited degrees of freedom. From the theoretical viewpoint, nulling with selected aperture elements can produce better results than either subarraying method. However, when the number of jammers is much less than the number of adaptive controls, all three techniques produce very good results.

Symmetry seems to be an important consideration when reducing the degrees of freedom. Symmetrical adaptive elements and subarrays limit distortions to the quiescent far field patterns. Unsymmetrical configurations tend to "fill in" the pattern's nulls. Any symmetrical arrangement produces real values for the far field pattern. The real cancellation beam and real quiescent pattern periodically add and subtract to give distinct nulls and peaks. Unsymmetrical configurations p produce complex cancellation beams. Adding together the quiescent pattern and cancellation beam produces a pattern with few distinct nulls. Thus, the sidelobes of the new far field pattern appear very distorted.

Analyzing the cancellation beams provides insite to the nulling process. Both subarraying techniques had cancellation beams with high gain in the direction of the quiescent pattern's main beam. The more jammers in the environment, the bigger the gain of the cancellation beam. Henee, the antenna's gain degraded. When nulling was performed with selected elements, the peak of the cancellation beam was in the direction of the interferenee. In this way, little gain was taken away from the main beam.

MISSION
of
Rome Air Development Center

RADC plans and executes research, development, test and selected acquisition programs in support of Command, Control Communications and Intelligence (C^3I) activities. Technical and engineering support within areas of technical competence is provided to ESD Program Offices (POs) and other ESD elements. The principal technical mission areas are communications, electromagnetic guidance and control, surveillance of ground and aerospace objects, intelligence data collection and handling, information system technology, ionospheric propagation, solid state sciences, microwave physics and electronic reliability, maintainability and compatibility.

Printed by
United States Air Force
Hanscom AFB, Mass. 01731


DAT
ILM